Computational Aeroacoustics : From Acoustic Sources Modeling to Far-Field Radiated Noise Prediction
Colloquium EUROMECH 449, December 9 – 12, 2003, Chamonix, France

An acoustic analogy applied to incompressible flow fields

Jonas Ask[*], Lars Davidson[**], Hans Enwald[*] and Johan Larsson[***]
[*] *Volvo Car Corporation, Fluid Dynamic Center , SE-405 31 Göteborg, Sweden*

[**] *Division of Thermo and Fluid Dynamics, Chalmers University of Technology, SE-412 96 Göteborg, Sweden*

[***] *Department of Mechanical Engineering University of Waterloo, Canada*

For low Mach number flows where walls are present the dominating source terms in Lighthill-Curle's equation are terms involving the wall pressure fluctuations. Since these terms are mainly affected by hydrodynamic phenomena one can assume that the sound sources can be captured in an incompressible flow field. This can only be carried out if the Lighthill-Curle's equation is kept in its compressible form. The assumption is then made that the source terms from the incompressible field are approximately the same as the corresponding sources from the compressible field.

In this work a modified version of the Lighthill-Curle's analogy is applied to study the near field acoustics of a laminar flow past an open cavity at a Mach number of 0.15 *with the length-to-depth ratio of* $L/D = 4$*. Three incompressible cases have been conducted and are compared against the corresponding compressible results. The three incompressible cases are carried out with different time-step sizes, distances from the cavity trailing edge to the outlet and spatial resolution in the stream wise direction. The aim of the work is to study the differences in compressible and incompressible sources to Lighthill-Curle's equation and their influence on the radiated sound which is a work in progress.*

Introduction

The field Computational Aero Acoustics (CAA) has during the last decade developed from a rather strict aeronautical field to include applications such as high speed trains and passenger cars. The intention with this work is to study to what degree these methods can be applied to traditional incompressible CFD. In this text traditional CFD will apply to convective boundary conditions and second order schemes. This work focuses thus at differences in compressible and incompressible sources to Lighthill-Curle's equation and their influence on the radiated sound.

The basic assumption is that the density fluctuations can be neglected for low Mach number flows. The sound generation and propagation can then be estimated by the sources evaluated from an incompressible flow field. This is only possible if Lighthill-Curle's equation is kept in its compressible form. The assumption is then that the difference between the sources predicted from a compressible and an incompressible flow field is negligible.

The method is based on a two step procedure for evaluating the sound pressure level at an observer point. The first step is based on extracting information from a transient incompressible CFD solution. In this case the two dipole source terms include the instantaneous wall pressure and the temporal wall pressure derivative. These terms have in previous works [7] been identified as the two dominating terms and are the only two terms treated in this work. This is true if pulsating leakages are not present.

The flow field

The investigated case is a laminar flow over an open cavity at a $Re_D = 1500$ based on the cavity depth and the free stream velocity and a corresponding Mach number of 0.15. At these conditions the flow in the cavity oscillates in "wake mode" defined in [2]. This mode is characterized by violent ejections of vortices from the cavity with length scales comparable with the cavity dimensions rather than the thickness of the boundary layer. The ejected vortex admits the free stream fluid to enter the cavity impinging on the downstream face of the cavity and triggers another vortex at the cavity leading edge. The vortex grows in the cavity until it completely fills the cavity and again gets ejected and triggers the next vortex shedding. The rapid changes in the flow past the cavity and its adjacent walls are the primary sources to generate sound. Additional studies treating these phenomena occurring in laminar flows over open cavities can be found in [3–7].

The solver used for this purpose is the incompressible FVM code CALC-BFC [8] with a second

order spatial Van Leer scheme for the convective fluxes in combination with a second order Crank-Nickolson time marching scheme. The pressure is coupled to the velocity field through the SIMPLEC pressure correction algorithm and the computational mesh is based on a single block arrangement with blockage outside the fluid domain.

The following boundary conditions are used: Symmetry at the far field boundary and no slip condition at the walls. Predefined velocity profiles for U and V at the inlet, extracted from an averaged compressible inflow profile 4.285D upstream the cavity leading edge. A disadvantage is that the inlet is very close to the cavity leading edge, forcing the naturally unsteady velocity profile to turn to an average profile. At the outlet a convective boundary condition is applied making it possible to shorten the distance to the outlet compared to a zero gradient boundary condition.

The investigated parameters for the different cases are presented in Table 1 below.

Parametric studies			
Case	dt	Cavity to outlet	Nodes in X-dir
ref	**0.001**	**15D**	**1270**
1	0.001	10D	460
2	0.005	15D	900
3	0.001	15D	900

Table 1 Parameter changes for the different cases

The case "ref" in Table 1 is the validating compressible reference case. More information regarding methodology, boundary conditions and discretization schemes for this case can be found in [1]. In Fig. 1 the geometrical dimensions of the domain is presented for case 1.

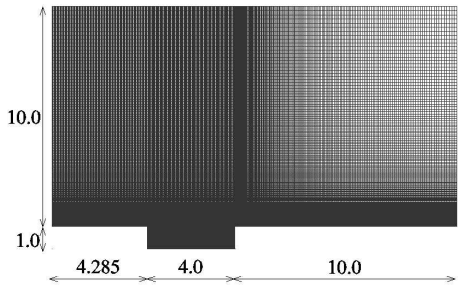

Fig. 1 Geometrical dimensions for case 1

Starting with the results from the flow field, the total cavity drag over one period is presented in Fig. 2 for the reference case and case 1. As can be seen from Fig. 2 the ejection of the large vortex structures generates rapid changes in the cavity drag. The lowest value occurs at the point when the vortex starts its travel out of the cavity causing a low pressure zone at the cavity downstream face. The

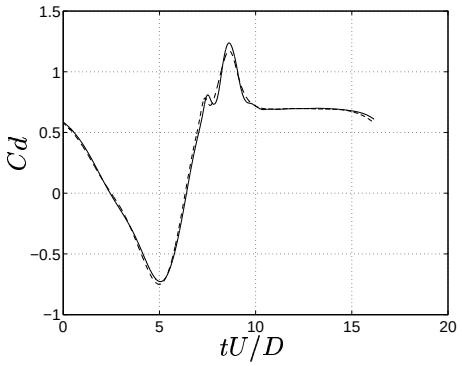

Fig. 2 C_D over one period

maximum peak in the cavity drag occurs when the vortex completely has left the cavity and is positioned approximately one cavity depth downstream the trailing edge exposing the downstream cavity face to the free-stream. The result is similar for the two other incompressible cases and the largest discrepancy in total drag for the presented cases can be found in the interval $7 < \frac{tU_\infty}{D} < 9.5$ when the vortex is being ejected.

The fundamental frequency in terms of the Strouhal number based on the cavity length and the oscillation periodicity is defined as:

$$St_L = \frac{fL}{U_\infty} \tag{1}$$

The results from case 1 to case 3 show a span in the Strouhal number where the highest value $St = 0.248$, occurs in case 1 and the lowest value $St = 0.245$, can be found in case 3. The value for case 2 is $St = 0.246$ and the corresponding reference case shows to be the same as for case 3, that is $St = 0.245$. Based on the three cases the time-step size and the domain length have weak influence on the fundamental frequency.

The acoustic field

A modified version of Lighthill-Curle was derived in [1] with the temporal derivatives inside the integral instead of keeping the spatial derivatives outside the integral as Curle's [9] original formulation states.

$$p(\mathbf{x},t) - p_o = \frac{1}{4\pi}\int_V \left[\frac{l_i l_j}{a_\infty^2 r}\ddot{T}_{ij} + \frac{3l_i l_j - \delta_{ij}}{a_\infty r^2}\dot{T}_{ij} + \frac{3l_i l_j - \delta_{ij}}{r^3}T_{ij}\right] dV(\mathbf{y}) + \frac{1}{4\pi}\int_S l_i n_j \left[\frac{\dot{p}\delta_{ij} - \dot{\tau}_{ij}}{a_\infty r} + \frac{p\delta_{ij} - \tau_{ij}}{r^2}\right] dS(\mathbf{y}) \tag{2}$$

Eq. 2 is valid for three dimensions while the flow field is computed in two dimensions. This is solved by expanding the solution in the span wise direction. A sensitivity study of this expansion was conducted in [7].

The instantaneous wall pressure is stored in the incompressible CFD solution and is used to reconstruct the second source term treated in this work. The two dipole source terms will in the following text use the index presented in Table 2, both are computed with second order accuracy in time and space.

Term index, l	Source term
1	$\frac{\partial p}{\partial \tau}\mid_w$
2	$p\mid_w$

Table 2 Treated source terms

In Figs. 3 and 4 the wall source intensity for the reference case and the three incompressible cases are presented. The source intensity is defined as

$$S_l = 20log_{10}\frac{\phi_{l,rms}}{\phi_{l,ref}} \tag{3}$$

where, $\phi_{l,ref} = \sqrt{\rho_\infty a_\infty 10^{-12} W/m^2}$ and the subscript l represents the source term index. In the two figures the geometry is fold out to visualize the results over the two vertical walls and are not to be mixed up with the actual computational geometry presented in Fig.1.

The wall source intensity at the inlet boundary differs approximately 2dB for term 2 between the reference case and the three incompressible cases. This deviation increases for term 1 indicating increased temporal pressure gradients. The levels are however at their lowest value at the inlet for both terms. The reason is as described in the text above most probably caused by the proximity of the inlet to the cavity leading edge and how the inlet boundary condition is applied. All incompressible cases show high levels in wall source intensity over the outlet. One reason is the instantaneous propagation of pressure disturbances caused by the boundary condition. In the cavity the wall source intensity is however in good agreement for all cases.

Radiated sound for 9 observers positioned at $-2.0D < x < 6.0D$, $y = 7.18D$, is presented in Fig. 5. The coordinate system has its origin at the cavity leading edge, 1D above the cavity bottom. Due to the different domain sizes the surface integration comprises the walls reaching from the inlet and to a distance of 10D downstream the cavity trailing edge.

The radiated sound for the presented cases show a maximum discrepancy of approximately 6 dB over the cavity trailing edge. The SPL for case 1 shows to be in better agreement with the reference case compared to case 2 and case 3. This result is in contradiction with the expectations and probable causes for this result are too coarse spatial resolution in the stream wise direction, a shorter domain, the applied boundary condition or a combination of above.

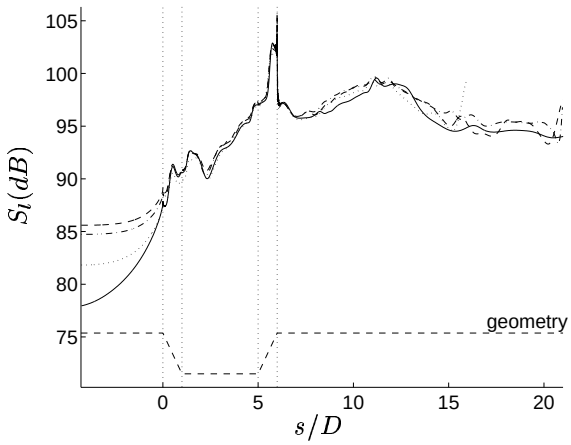

Fig. 3 Wall source intensity for term 1, (-) ref, (..) case 1, (- -) case 2, (.-) case 3

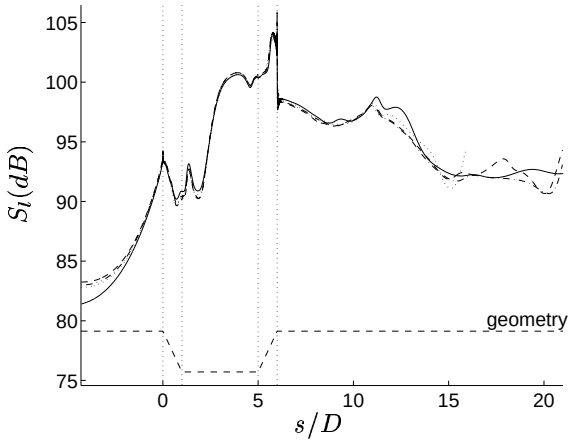

Fig. 4 Wall source intensity for term 2, (-)ref, (..)case 1, (- -) case 2, (.-)case 3

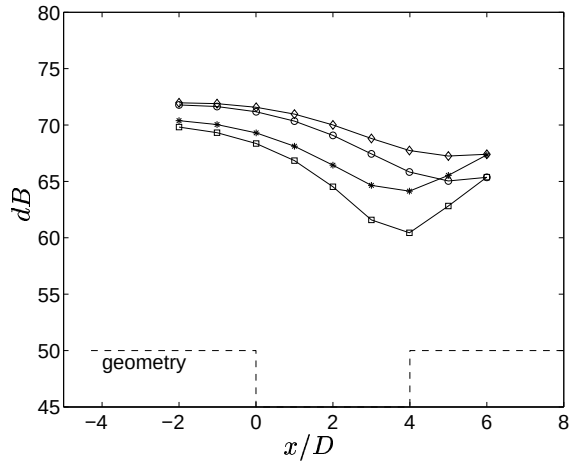

Fig. 5 SPL for observers, $-2.0D < x > 6.0D$, $y = 7.18D$, □ ref, ⋆ case 1, ◇ case 2, ○ case 3

The effect of the domain size is investigated through a sensitivity study of the surface integration for observer $x = 4D$, $y = 7.18D$ in case 3 and the reference case. The result presented in Fig. 6 shows the changes in SPL when the integrated surface gradually is increased from 10D downstream the cavity trailing edge to a distance of 15D by a

step increment of 1D. As can be seen from the result no major changes in the SPL was found indicating that the deviation in Fig. 5 is not a consequence of local cancellation effects.

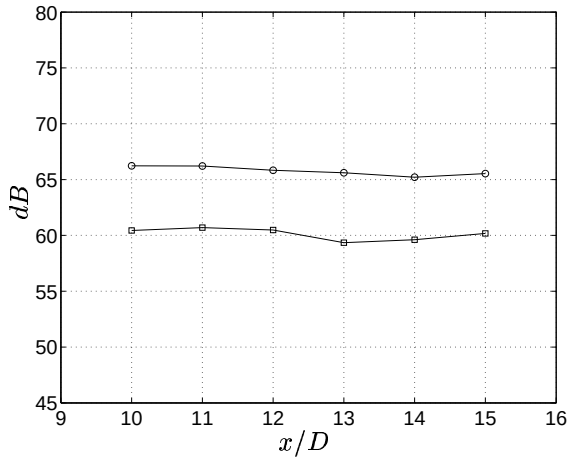

Fig. 6 SPL at $x = 4D$, $y = 7.18D$, □ ref, ∘ case 3.

If the surface integration is limited to the three walls in the cavity, the radiated sound for the same observers shows to be within 1dB for all cases, Fig. 7. This indicates that the noise generating mechanisms in the cavity is equally resolved in the incompressible cases as in the reference case. However, the resolution might still be an issue outside the cavity.

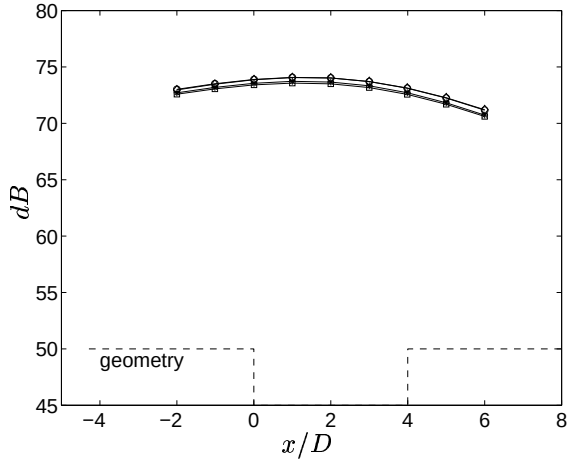

Fig. 7 SPL in observers, $-2.0D < x > 6.0D$, $y = 7.18D$, □-ref, ⋆ case 1, ⋄ case 2, ∘ case 3

The radiated sound is highly influenced by the wall source strength, the phase of the sources and the domain size. In Figs. 3 and 4 the wall source strength show good agreement between the cases except at the in and outlet. When the domain is reduced to only contain the cavity walls even the radiated sound is in an almost perfect match, Fig. 7. One possible explanation to the result in Fig. 5 is that the phase of the sources outside the cavity is incorrect. But the most probable cause to the results found in this work is the lack of a buffer layer at the outlet. The effect of a buffer layer at the outlet is currently being investigated.

Conclusion

As mentioned above this is a work in progress and an overall conclusion can not be drawn before the reflections from the outlet are eliminated. However, the following observations are noticed. Both inlet and outlet in the incompressible cases is of reflective character. The inlet due to the applied average velocity profiles in U and V close to the cavity leading edge. This restricts the instantaneous flow field and results in unphysical pressure gradients. The outlet is highly reflective. One solution to this problem is to move the outlet further downstream with increased calculation time as a result. Another more effective solution might be to introduce buffer layers over the outlet as is customary in the compressible CAA field.

Acknowledgment

This work is a part of a project called "Computational Aero Acoustics for Vehicle Applications" funded by VINNOVA and Volvo Car Corporation. The project is a collaboration project between Chalmers University of Technology and Volvo Car Corporation.

Johan Larsson has contributed with the compressible database and the two other contributors to this work are the academic and industrial supervisor.

References

[1] Larsson, J., Davidsson, L., Olsson, M., and Eriksson, L.-E., "Aero acoustic investigation of an open cavity at low Mach number," *AIAA/CEAS Aeroacoustics Conference and Exhibit*, 2003, pp. AIAA–2003–3237.

[2] Gharib, M. and Roshko, A., "The effect of flow oscillations on cavity drag," *Journal of Fluid Mechanics*, Vol. 177, 1987, pp. 501–530.

[3] Colonius, T., "An overview of simulation, modeling and active control of flow/acoustic resonance in open cavities," *AIAA/CEAS Aeroacoustics Conference and Exhibit*, 2001, pp. AIAA–2001–0076.

[4] Colonius, T., Basu, A. J., and Rowley, C. W., "Computaion of sound generation and flow/acoustic instabilities in the flow past an open cavity," *3rd ASME/JSME Joint Fluids Engineering Conference*, 1999, pp. FEDSM99–7228.

[5] Rowley, C. W., Colonius, T., and Basu, A. J., "On self-sustained oscillations in two-dimensional compressible flow over rectangular cavities," *Journal of Fluid Mechanics*, Vol. 455, 2002, pp. 315–346.

[6] Gharib, M., "Response of the cavity shear layer oscillations to external forcing," *AIAA Journal*, Vol. 25, 1987, pp. 43–47.

[7] Larsson, J., "Computational Aero Acoustics for Vehicle Applications," Chalmers University of Technology, 2002.

[8] Davidsson, L. and Farhanieh, B., "CALC-BFC, A Finite-Volume Code Employing Collocated Variable Arrangement and Cartesian Velocity Components for Computation of Fluid Flow and Heat Transfer in Complex Three-Dimensional Geometries," Chalmers University of Technology, Department of Thermo and Fluid Dynamics, 1995.

[9] Curle, N., "The influence of solid boundaries upon aerodynamic sound," *Proc. Roy. Soc*, Vol. A231, 1955, pp. 505–514.